A Theoretical Comparison of the Breakdown Behavior of $In_{0.52}Al_{0.48}As$ and InP Near-Infrared Single-Photon Avalanche Photodiodes

Souye Cheong Liew Tat Mun, Chee Hing Tan, *Member, IEEE*, Simon J. Dimler, Lionel J. J. Tan, Jo Shien Ng, *Member, IEEE*, Yu Ling Goh, *Student Member, IEEE*, and John P. R. David, *Senior Member, IEEE*

***Abstract*—We study the breakdown characteristics and timing statistics of InP and $In_{0.52}Al_{0.48}As$ single-photon avalanche photodiodes (SPADs) with avalanche widths ranging from 0.2 to 1.0 μm at room temperature using a random ionization path-length model. Our results show that, for a given avalanche width, the breakdown probability of $In_{0.52}Al_{0.48}As$ SPADs increases faster with overbias than InP SPADs. When we compared their timing statistics, we observed that, for a given breakdown probability, InP requires a shorter time to reach breakdown and exhibits a smaller timing jitter than $In_{0.52}Al_{0.48}As$. However, due to the lower dark count probability and faster rise in breakdown probability with overbias, $In_{0.52}Al_{0.48}As$ SPADs with avalanche widths $\leq$ 0.5 μm are more suitable for single-photon detection at telecommunication wavelengths than InP SPADs. Moreover, we predict that, in InP SPADs with avalanche widths $\leq$ 0.3 μm and $In_{0.52}Al_{0.48}As$ SPADs with avalanche widths $\leq$ 0.2 μm, the dark count probability is higher than the photon count probability for all applied biases.**

***Index Terms*—Avalanche breakdown, InP, $In_{0.52}Al_{0.48}As$, single-photon avalanche photodiodes (SPADs), timing statistics.**

I. Introduction

Geiger-MODE avalanche photodiodes (APDs), commonly known as single-photon avalanche diodes (SPADs), have recently emerged as a key technology for applications requiring single-photon detection such as in quantum key distribution systems [1], in time-of-flight laser ranging applications [2], and in time-resolved photon counting [3]. While linear-mode InP and $In_{0.52}Al_{0.48}As$-based APDs have been characterized extensively [4]–[9] for applications at the telecommunication wavelength of 1.55 μm, their performance in geiger-mode has not yet been fully optimized. Since the early studies by Oldham *et al.* [10] and by McIntyre [11] on the breakdown characteristics of SPADs, several works have significantly contributed to the understanding of the dynamics in SPADs.

Using a history-dependent analytical model, Wang *et al.* [12] suggested that a faster increase in breakdown probability with overbias ratio, $P_b(V_{\text{over}})$, can be achieved in $In_{0.52}Al_{0.48}As$ diodes than in InP diodes while Ng *et al.* studied the effects of deadspace [13] and field dependences of ionization coefficient ratio [14] on the rate at which $P_b(V_{\text{over}})$ increases using a hard deadspace model. In [13] and [14], these authors found that a large dead-space-to-avalanche-width ratio and a large ionization coefficient ratio leads to faster increase in $P_b(V_{\text{over}})$. Ramirez *et al.* [15] investigated a set of design parameters using the recursive deadspace multiplication model [16] and showed that a larger increase in $P_b(V_{\text{over}})$ is achieved using InP and $In_{0.52}Al_{0.48}As$ SPADs with thicker avalanche width. Interestingly, they also found the single-photon quantum efficiency (SPQE), a figure of merit incorporating the dark count probability, the photon count probability, and the probability that there is at least one photon during the gated time, to be higher in InP SPADs than in $In_{0.52}Al_{0.48}As$ SPADs for a given avalanche width. However, these works [12]–[15] relied on ionization coefficients derived using limited experimental data. Moreover, their analysis omitted timing statistics which are critical in applications where the timing resolution can be the limiting factor to the photon detector's performance.

When APDs are biased to a metastable condition, a single absorbed photon can initiate breakdown, and the time taken for the avalanche current to build up to the circuit threshold current depends on the ionization process. This process is stochastic in nature, hence, creating a spread in the time taken to breakdown, commonly termed as the timing jitter. Spinelli *et al.* [17] investigated the timing statistics of Si SPADs and they concluded that diffusion-assisted process dominates the timing statistics. Using a random path length (RPL) model, Tan *et al.* [18] later demonstrated that these timing statistics are also affected by deadspace and ionization coefficient ratios. They showed that, in materials with similar ionization coefficients and having low deadspace contribution, the time taken to reach breakdown is low and the timing jitter is small.

In this study, we compare the timing statistics of InP and $In_{0.52}Al_{0.48}As$ SPADs at room temperature using a RPL model that employs ionization coefficients derived from a wide range of devices for these two materials and that is similar to the model used in [18]. We also study the competing effects of the increase in dark count due to tunneling current and photon count whilst the timing jitter decreases as the avalanche width is reduced. This model has been shown to be accurate in modeling the avalanche breakdown voltage of APDs [19] and is equivalent

Manuscript received May 27, 2008; revised August 14, 2008. Current version published April 17, 2009.

The authors are with the Department of Electronic and Electrical Engineering, University of Sheffield, Sheffield S1 3JD, U.K. (e-mail: s.liew-tat-mun@shef.ac.uk; c.h.tan@shef.ac.uk; s.dimler@shef.ac.uk; lionel.tan@shef.ac.uk; j.s.ng@shef.ac.uk; elp03ylg@shef.ac.uk; j.p.david@shef.ac.uk).

Digital Object Identifier 10.1109/JQE.2009.2013094

0018-9197/$25.00 © 2009 IEEE

to models based on solving the recurrence equations as demonstrated in [18]. Moreover, the model has been demonstrated to give comparable avalanche breakdown current features to those calculated in full band Monte Carlo model [20].

II. Model

The RPL model uses the ionization path-length probability density functions (PDFs) as input parameters to calculate the ionization probability. Under constant electric fields, these electron PDFs can be described analytically as

$$h_e(x_e) = \begin{cases} 0, & x_e < d_e \\ \alpha^* \exp\left[-\alpha^*(x_e - d_e)\right], & x_e \geq d_e \end{cases} \quad (1)$$

where d_e represents the electron deadspace, α^* is the enabled electron ionization coefficient, and x_e represents the electron ionization path length. A similar expression for the hole PDFs is obtained by replacing d_e, α^*, and x_e with d_h, β^*, and x_h respectively. Further details on the RPL model can be found in [18]–[20]. In our calculations, we used $In_{0.52}Al_{0.48}As$ and InP ionization coefficients and threshold energies published in [7] and [9], respectively, as these parameters were derived using multiplication and excess noise factors measured on a series of devices covering a wide range of electric fields using pure electron and pure hole injection. Hence, we believe that [7] and [9] provide the most reliable ionization coefficients and parameters to date.

To calculate the avalanche current I, we used Ramo's theorem [21], which is given by $I = qv_s/w$, where q is the electronic charge, w is the avalanche width, and v_s is the saturated velocity. We assumed v_s values of 1.0×10^5 ms^{-1} for electrons and 6.0×10^4 ms^{-1} for holes for both InP and $In_{0.52}Al_{0.48}As$. As a result, the timing statistics obtained was solely functions of w, ionization coefficient ratio, and deadspace. In our simulation, the circuit threshold current was set to 50 μA, the breakdown probability P_b was calculated as the ratio of the number of carriers triggering breakdown to the number of injected carriers, the mean time to breakdown t_b was taken as the mean time required for the avalanche current to reach the circuit threshold current, and the timing jitter σ was taken as the standard deviation of the mean time to breakdown. Interestingly, we found that using higher threshold current does not affect σ obtained for a given w but merely increases t_b as previously observed by Groves *et al.* [22]. To achieve convergence of our results, 6×10^4 particles were simulated. In this study, the electric field was assumed to remain constant as the avalanche current builds up.

In real SPADs, the timing jitter can arise as a result of the random position of the absorbed photon in the absorption layer and from the random impact ionization events occurring during avalanche breakdown. As both InP and $In_{0.52}Al_{0.48}As$ SPADs have InGaAs as their absorption layer, the timing jitter resulting from the former process is expected to be similar in both SPADs for a given InGaAs absorption layer. Thus, to compare the timing statistics occurring due to the ionization events in InP and $In_{0.52}Al_{0.48}As$ multiplication layers, we simulated breakdown events in ideal $p^+ - i - n^+$ and $n^+ - i\text{-}p^+$ structures with w = 0.20, 0.30, 0.40, 0.50 and 1.0 μm. Due to the different majority ionizing carriers in these materials, pure electrons were injected into the p^+ side of the multiplication layer for $In_{0.52}Al_{0.48}As$ while pure holes were injected into the n^+ side of the multiplication layer for InP. As for the dark carriers, we assumed that they are generated uniformly and randomly in the avalanche region during the gated time.

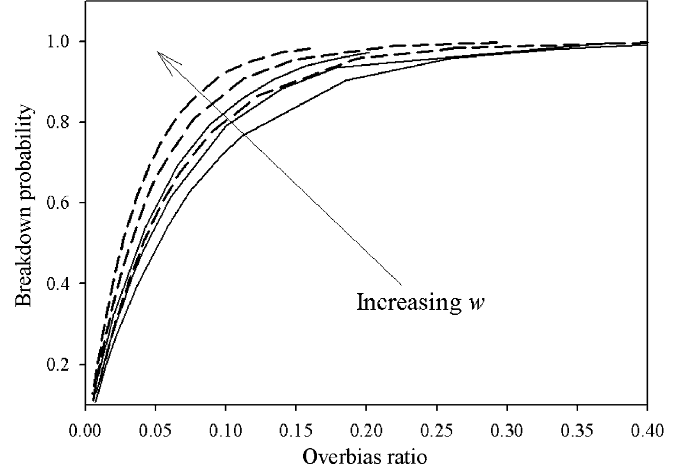

Fig. 1. Calculated breakdown probability for $In_{0.52}Al_{0.48}As$ (---) and InP (—) as a function of overbias ratio for SPADs with w of 0.20, 0.50, and 1.00 μm. The results for SPADs with w of 0.30 and 0.40 μm are not shown for clarity.

III. Results and Discussion

Fig. 1 shows the calculated breakdown probability as a function of overbias ratio, defined as $V_{\text{over}} = (V - V_{\text{BR}})/V_{\text{BR}}$, where V is the applied bias and V_{BR} is the breakdown voltage, assumed to be the voltage that yields a breakdown probability of 0.001. At a given overbias ratio, the thickest diode produces the largest breakdown probability. Our results also show that $In_{0.52}Al_{0.48}As$ diodes exhibit a larger increase in $P_b(V_{\text{over}})$ than InP diodes for a given w, confirming the trend obtained by Wang *et al.* [12] and Ramirez *et al.* [15] despite the different ionization coefficients and threshold energies used.

McIntyre [11] showed that $P_b(V_{\text{over}})$ rises more rapidly in diodes with large ionization coefficient ratio while Ng *et al.* [13] demonstrated, and later confirmed by Tan *et al.* [20], that larger deadspace also leads to a more rapid rise in $P_b(V_{\text{over}})$. Thus, to assess the dominant effect that is causing the more rapid rise in $P_b(V_{\text{over}})$ in $In_{0.52}Al_{0.48}As$ diodes, we compared the ionization coefficient ratio of InP and $In_{0.52}Al_{0.48}As$ as a function of breakdown probability in Fig. 2. For a given w, it is evident that the electron-to-hole ionization coefficient ratio in $In_{0.52}Al_{0.48}As$ is larger than the hole-to-electron ionization coefficient ratio in InP. As expected, in the thinnest diode and at high breakdown probabilities, the difference between the two ratios reduces as a result of the convergence of ionization coefficients at high electric fields. We then assessed the ratio of deadspace d calculated as $d = E_{\text{th}}/q\varepsilon$ where E_{th} is the threshold energy and ε the electric field, to w for each diode. As pure electrons were injected for $In_{0.52}Al_{0.48}As$ SPADs and pure holes for InP SPADs, Fig. 3 compares the calculated

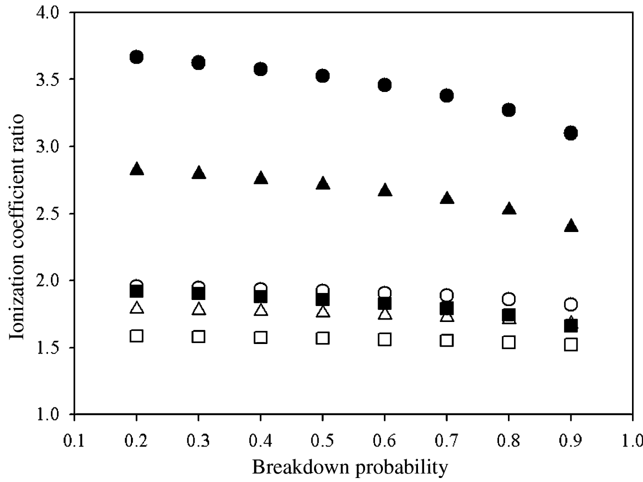

Fig. 2. Ionization coefficient ratios for InP (open symbols) and $In_{0.52}Al_{0.48}As$ (closed symbols) calculated as a function of breakdown probability for SPADs with w of 0.20 (□, ■), 0.50 (△, ▲), and 1.00 μm (∘, •). The results for SPADs with w of 0.30 and 0.40 μm are not shown for clarity.

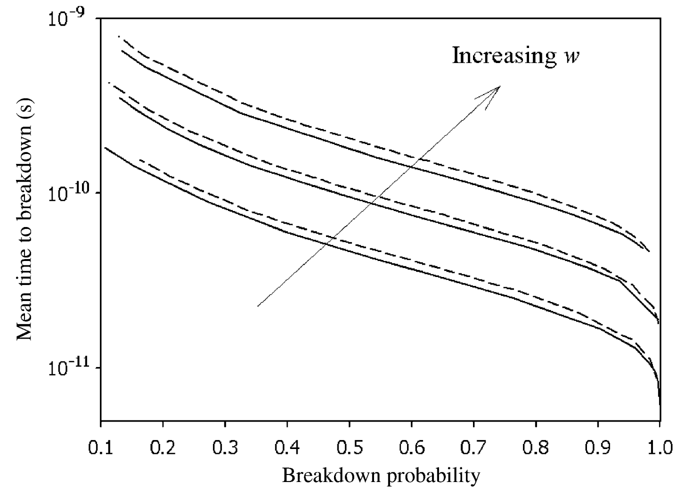

Fig. 4. Calculated mean time to breakdown for $In_{0.52}Al_{0.48}As$ (- - -) and InP (—) as a function of breakdown probability for SPADs with w of 0.20, 0.50 and 1.00 μm. The results for SPADs with w of 0.30 and 0.40 μm are not shown for clarity.

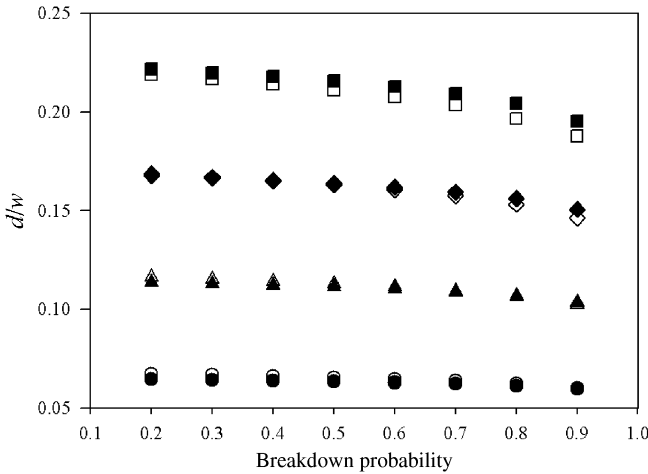

Fig. 3. Deadspace-to-avalanche-width ratio for InP (open symbols) and $In_{0.52}Al_{0.48}As$ (closed symbols) calculated as a function of breakdown probability for SPADs with w of 0.20 (□, ■), 0.30 (◇, ◆), 0.50 (△, ▲), and 1.00 μm (∘, •). The results for diodes with w of 0.40 μm are not shown for clarity.

d_e/w for $In_{0.52}Al_{0.48}As$ and d_h/w for InP as a function of the breakdown probability. Interestingly, we can observe that, in SPADs with $w \leq 0.3\ \mu$m, the contribution of deadspace is more significant in $In_{0.52}Al_{0.48}As$ than in InP but, as w increases, an opposite behavior is observed; the deadspace becomes more significant in InP than in $In_{0.52}Al_{0.48}As$. However, as the difference in d/w values between InP and $In_{0.52}Al_{0.48}As$ is not significant for a given breakdown probability, our results therefore suggest that the steeper rise in $P_b(V_{\text{over}})$ observed for $In_{0.52}Al_{0.48}As$ is caused by the more pronounced effect of the larger ionization coefficient ratio than that of the deadspace effect.

When the values of t_b calculated for InP and $In_{0.52}Al_{0.48}As$ SPADs were compared in Fig. 4, we observed smaller values in InP than in $In_{0.52}Al_{0.48}As$ for a given w. Moreover, the lowest t_b was obtained in the thinnest diodes. These timing results can be explained by the shorter transit time combined with the effects of the ionization coefficient ratio and deadspace, as previously discussed by Tan *et al.* [18]. These authors showed analytically that the lowest t_b is obtained in thin diodes having similar electron and hole ionization coefficients and small deadspace effect. As shown earlier, for a given breakdown probability, InP has a smaller ionization coefficient ratio and similar d/w when compared with $In_{0.52}Al_{0.48}As$, resulting in the smaller t_b for InP SPADs. Moreover, the values of t_b recorded for $In_{0.52}Al_{0.48}As$ SPADs is found to be approximately 12% longer than those recorded for InP SPADs for a given w. However, the exact difference between the values of t_b for real diodes will not only be dependent on the saturation velocities, ionization coefficients ratio, and deadspace contribution but also on the effect of the enhanced velocity occurring in early ionizing carriers [18] and on the space charge effect [17].

The values of σ calculated for InP and $In_{0.52}Al_{0.48}As$ SPADs are shown in Fig. 5. As expected, we observed that diodes having the smallest w produce the lowest σ for a given avalanche material, which is consistent with the findings of [18]. When the two materials were compared, InP shows a smaller σ than $In_{0.52}Al_{0.48}As$ for a given w due to the smaller ionization coefficients ratio in InP. Moreover, we obtained the difference in σ values between InP and $In_{0.52}Al_{0.48}As$ SPADs to be approximately equal to 18% for all w. However, as commercially available time-to-amplitude converter (TAC) equipment [23] has at best, a timing resolution of 7 ps, the smaller σ in InP SPADs does not always provide significant timing advantages. As the timing jitter of the SPAD and the timing resolution of the TAC σ_{TAC} are independent of each other, the combined timing jitter σ_t would be measured as $\sigma_t^2 = \sigma^2 + \sigma_{TAC}^2$. For instance, in SPADs with $w = 0.2\ \mu$m and operating at a breakdown probability of 0.5, InP and $In_{0.52}Al_{0.48}As$ SPADs exhibit σ values of 9.8 and 11.5 ps, which would yield σ_t values of 12.0 and 13.5 ps, respectively. Therefore, the difference in σ between the two materials decreases from 18.0% to 12.5% for these SPADs, suggesting that the difference could become

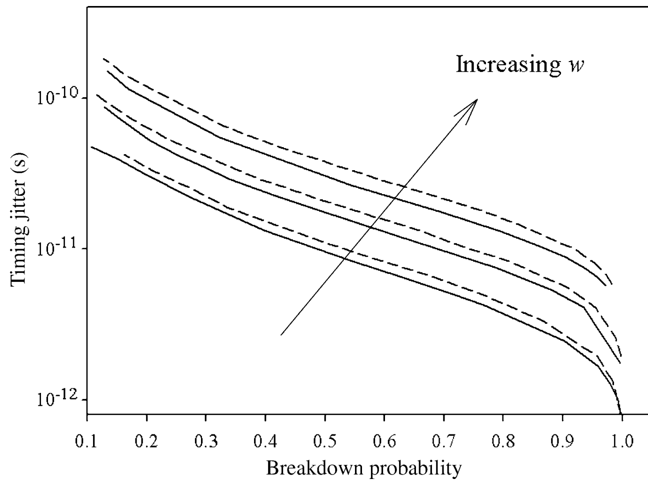

Fig. 5. Calculated timing jitter for $In_{0.52}Al_{0.48}As$ (---) and InP (—) as a function of breakdown probability for SPADs with w of 0.20, 0.50, and 1.00 μm. The results for SPADs with w of 0.30 and 0.40 μm are not shown for clarity.

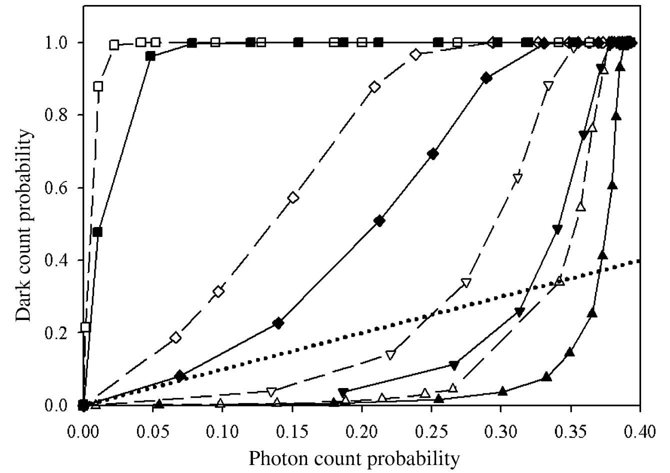

Fig. 7. Dark count probability calculated as a function of photon count probability for InP (open symbols) and $In_{0.52}Al_{0.48}As$ (closed symbols) SPADs with w of 0.20 (□, ■), 0.30 (◇, ◆), 0.40 (▽, ▼), and 0.50 μm (△, ▲). Lines associated with the symbols are plotted to assist visualization. The line (●●●) shows the condition where the dark count probability is equal to the photon count probability.

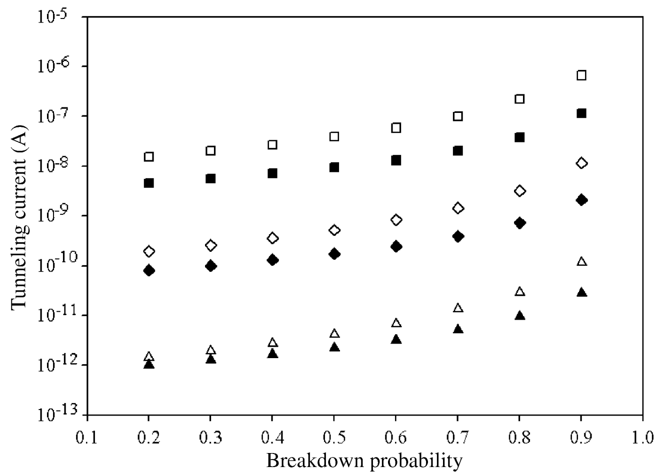

Fig. 6. Tunneling current calculated for circular SPADs with radius of 10 μm for InP (open symbols) and $In_{0.52}Al_{0.48}As$ (closed symbols) as a function of breakdown probability for SPADs with w of 0.20 (□, ■), 0.30 (◇, ◆), and 0.50 μm (△, ▲). The results for SPADs with w of 0.40 μm are not shown for clarity.

less significant depending on the applications and limitations of existing measuring apparatus.

In SPADs, besides P_b, t_b, and σ, it is also crucial to analyze the dark counts. As Karve *et al.* [24] suggested, band-to-band tunneling in the multiplication layer of thin SPADs can contribute to the majority of dark counts. Thus, in order to assess the dark count rates of InP and $In_{0.52}Al_{0.48}As$, we analyzed the tunneling currents of SPADs having $w \leq 0.5$ μm. In our calculation, the band-to-band tunneling current $I_{\rm tun}$ was calculated using experimentally derived tunneling parameters for $In_{0.52}Al_{0.48}As$ [6] and InP [9] for diodes having circular mesas and radius of 10 μm. As shown in Fig. 6, InP exhibits higher tunneling current than $In_{0.52}Al_{0.48}As$ for a given breakdown probability, suggesting a higher number of dark carriers in InP. Interestingly, this observation is in contradiction to that predicted by Ramirez *et al.* [15] who approximated the tunneling current of InP using parameters derived for $In_{0.52}Al_{0.48}As$. As a result, these authors underestimated the tunneling current in InP SPADs.

For most single-photon detection applications, low dark count and high photon count are desirable. Thus, we calculated the photon count probability and the dark count probability in InP and $In_{0.52}Al_{0.48}As$ SPADs with $w \leq 0.5$ μm using Poissonian statistics for a given set of conditions. The dark count probability was calculated as $1 - \exp(-N_d P_d)$ [25], where P_d is the breakdown probability of dark carriers generated randomly in the avalanche region and N_d is the number of dark carriers during the on-time given as $N_d = I_{\rm tun} \times t_{\rm gated}/q$ where $t_{\rm gated}$ is the gated time and taken as 2 ns in this study. As for the photon count probability, we assumed that all carriers generated by photons absorbed in the absorption layer reach the multiplication layer. Therefore, the photon count probability was calculated as $1 - \exp(-\eta N_0 P_b)$, where η is the quantum efficiency taken as 0.5 and N_o is the number of photon per pulse taken as 1. As shown in Fig. 7, $In_{0.52}Al_{0.48}As$ has a lower dark count probability than InP for a given photon count probability. Interestingly, we also observed that, in InP SPADs with $w \leq 0.3$ μm and $In_{0.52}Al_{0.48}As$ SPADs ≤ 0.2 μm, the dark count probability is always larger than the photon count probability, suggesting that these diodes would be impractical for most single-photon applications. These observations are consistent with those reported by Ramirez *et al.* [15]. Moreover, as w increases, the range over which the probability of achieving higher photon count than dark count also increases. For instance, in InP SPADs with $w = 0.4$ and 0.5 μm, we obtained equal dark and photon count probabilities at photon count probabilities of 0.25 and 0.34, which correspond to overbias ratios of around 0.06 and 0.12, respectively. As for $In_{0.52}Al_{0.48}As$ SPADs with $w = 0.4$ and 0.5 μm, equal dark count and photon count probabilities were obtained for photon count probabilities of 0.32 and 0.37, which correspond to overbias ratios of around 0.07 and 0.13, respectively. These results

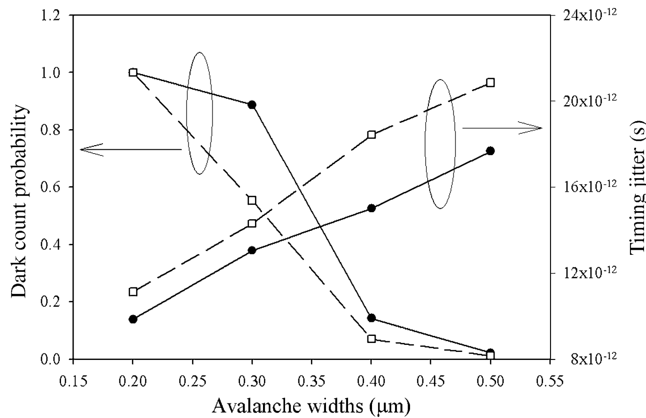

Fig. 8. Dark count probability and timing jitter calculated at a breakdown probability of 0.5 as a function of w for InP (•) and $In_{0.52}Al_{0.48}As$ (□). Lines associated with the symbols are guides to the eyes.

therefore suggest that, due to the lower dark count probability for a given photon count probability and the larger increase in $P_b(V_{\rm over})$ in $In_{0.52}Al_{0.48}As$ SPADs, these diodes would outperform InP SPADs for applications at the telecommunication wavelength despite their poorer timing statistics.

To study the performance of SPADs with w, Fig. 8 shows the dark count probability and σ calculated at a breakdown probability of 0.5 for different w. It can be seen that, as w increases, the dark count probability decreases. As tunneling current decreases exponentially with electric field, the lower electric field required to achieve a given breakdown probability in thicker SPADs yields smaller tunneling current, resulting in fewer dark carriers and hence smaller dark count probability. However, the same increase in w will cause t_b and σ to increase. Thus, as w increases, there exists a trade-off between σ and dark count probability for SPADs. A similar trade off between tunneling current and breakdown probability was also observed by Ramirez *et al.* [15].

IV. Conclusion

We have shown that InP SPADs has better timing characteristics than $In_{0.52}Al_{0.48}As$ SPADs assuming that these materials have similar saturated velocities. The lower values of t_b and σ observed in InP can be explained by the more pronounced effect of the ionization coefficient ratio than the deadspace effect. Moreover, we found that $In_{0.52}Al_{0.48}As$ SPADs with $w \leq 0.2\ \mu$m and InP SPADs with $w \leq 0.3\ \mu$m would be unsuitable for applications requiring larger photon count probability than dark count probability. As $In_{0.52}Al_{0.48}As$ SPADs exhibit a larger increase in $P_b(V_{\rm over})$, lower dark count probability and provide a larger range over which the ratio of photon to dark count probability exceeding 1, they will be more suited than InP SPADs for applications at telecommunication wavelengths despite their poorer timing statistics.

References

[1] D. Stucki, G. Ribordy, A. Stefanov, H. Zbinden, and J. G. Rarity, "Photon counting for quantum key distribution with Peltier cooled InGaAs/InP APDs," *J. Mod. Opt.*, vol. 48, no. 13, pp. 1967–1981, 2001.

[2] S. Pellegrini, G. S. Buller, J. M. Smith, A. M. Wallace, and S. Cova, "Laser based distance measurement using picosecond resolution time-correlated single-photon counting," *Meas. Sci. Technol.*, vol. 11, pp. 712–716, 2000.

[3] A. Spinelli, L. M. Davis, and H. Dautet, "Actively quenched single-photon avalanche diode for high repetition rate time-gated photon counting," *Rev. Sci. Instrum.*, vol. 67, pp. 55–61, 1996.

[4] F. Capasso, K. Mohammed, K. Alavi, A. Y. Cho, and P. W. Foy, "Impact ionization rates for electrons and holes in $Al_{0.48}In_{0.52}As$," *Appl. Phys. Lett.*, vol. 45, pp. 968–970, 1984.

[5] P. Yuan, C. C. Hansing, K. A. Anslem, C. V. Lennox, H. Nie, A. L. Holmes, B. G. Streetman, and J. C. Campbell, "Impact ionization characteristics of III-V. semiconductors for a wide range of multiplication region thickness," *IEEE J. Quantum Electron.*, vol. 36, no. 1, pp. 198–204, Jan. 2000.

[6] Y. L. Goh, D. J. Massey, A. J. R. Marshall, J. S. Ng, C. H. Tan, W. K. Ng, G. J. Rees, M. Hopkinson, J. P. R. David, and S. K. Jones, "Avalanche multiplication in InAlAs," *IEEE Trans. Electron Devices*, vol. 54, no. 1, pp. 11–16, Jan. 2007.

[7] Y. L. Goh, A. R. J. Marshall, D. J. Massey, J. S. Ng, C. H. Tan, M. Hopkinson, J. P. R. David, S. K. Jones, C. C. Button, and S. M. Pinches, "Excess avalanche noise in $In_{0.52}Al_{0.48}As$," *IEEE J. Quantum Electron.*, vol. 43, no. 6, 2007.

[8] L. J. J. Tan, J. S. Ng, C. H. Tan, M. Hopkinson, and J. P. R. David, "Effect of deadspace on low field avalanche multiplication in InP," *IEEE Trans. Electron Devices*, vol. 54, no. 8, pp. 2051–2054, Aug. 2007.

[9] L. J. J. Tan, J. S. Ng, C. H. Tan, and J. P. R. David, "Avalanche noise characteristics in sub-micron InP diodes," *IEEE. J. Quantum Electron.*, vol. 44, no. 4, pp. 378–382, Apr. 2008.

[10] W. G. Oldham, R. R. Samuelson, and P. Antognetti, "Triggering phenomena in avalanche diodes," *IEEE Trans. Electron Devices*, vol. ED-19, no. 9, pp. 1056–1060, Sep. 1972.

[11] R. J. McIntyre, "On the avalanche initiation probability of avalanche diodes above the breakdown voltage," *IEEE. Trans. Electron Devices*, vol. ED-20, no. 7, pp. 637–641, Jul. 1973.

[12] S. Wang, F. Ma, X. Li, G. Karve, X. Zheng, and J. C. Campbell, "Analysis of breakdown probabilities in avalanche photodiodes using a history-dependent analytical model," *Appl. Phys. Lett.*, vol. 82, pp. 1971–1973, 2003.

[13] J. S. Ng, C. H. Tan, G. J. Rees, and J. P. R. David, "Effects of dead space on breakdown probability in Geiger mode avalanche photodiode," *J. Mod. Opt.*, vol. 54, pp. 353–360, 2007.

[14] J. S. Ng, C. H. Tan, and J. P. R. David, "A comparison of avalanche breakdown probabilities in semiconductor materials," *J. Mod. Opt.*, vol. 51, pp. 1315–1321, 2004.

[15] D. A. Ramirez, M. M. Hayat, G. Karve, J. C. Campbell, S. N. Torres, B. E. A. Saleh, and M. C. Teich, "Detection efficiencies and generalized breakdown probabilities for nanosecond-gated near infrared single photon avalanche photodiodes," *IEEE J. Quantum Electron.*, vol. 42, no. 2, pp. 137–145, Feb. 2006.

[16] M. M. Hayat, U. Sakoglu, O. H. Kwon, S. Wang, J. C. Campbell, B. E. A. Saleh, and M. C. Teich, "Breakdown probabilities for thin heterostructure avalanche photodiodes," *IEEE J. Quantum Electron.*, vol. 39, no. 2, pp. 179–185, Feb. 2003.

[17] A. Spinelli and A. L. Lacaita, "Physics and numerical simulation of single photon avalanche diodes," *IEEE Trans. Electron Devices*, vol. 44, no. 11, pp. 1931–1943, Nov. 1997.

[18] C. H. Tan, J. S. Ng, G. J. Rees, and J. P. R. David, "Statistics of avalanche current build up time in single photon avalanche diodes," *IEEE J. Sel. Topics Quantum Electron.*, vol. 13, no. 4, pp. 906–910, Jul.–Aug. 2007.

[19] D. S. Ong, K. F. Li, G. J. Rees, J. P. R. David, and P. N. Robson, "A simple model to determine multiplication and noise in avalanche photodiodes," *J. Appl. Phys.*, vol. 83, pp. 3426–3428, 1998.

[20] S. L. Tan, D. S. Ong, and H. K. Yow, "Theoretical analysis of breakdown probabilities and jitter in single-photon avalanche diodes," *J. Appl. Phys.*, vol. 102, pp. 44506-1–44506-7, 2007.

[21] S. Ramo, "Currents induced by electron motion," *Proc. IRE*, pp. 584–585, 1992.

[22] C. Groves, C. H. Tan, J. P. R. David, G. J. Rees, and M. M. Hayat, "Exponential time response in analogue and geiger mode avalanche photodiodes," *IEEE Trans. Electron Devices*, vol. 52, no. 6, pp. 1527–1534, Jun. 2007.

[23] "Model 2145 Time to Amplitude Converter/Single channel Analyzer, Datasheet," Canberra [Online]. Available: http://www.canberra.com/pdf/Products/NIM_pdf/2145_SS.pdf

[24] G. Karve, S. Wang, F. Ma, X. Li, J. C. Campbell, R. G. Ispasoiu, D. S. Bethune, W. P. Risk, G. S. Kinsey, J. C. Boisvert, T. D. Isshiki, and R. Sudharsanan, "Origin of dark counts in $In_{0.53}Ga_{0.47}As/In_{0.52}Al_{0.48}As$ avalanche photodiodes operated in geiger mode," *Appl. Phys. Lett.*, vol. 86, pp. 63 505-1–63 505-3, 2005.

[25] O. H. Kwon, M. M. Hayat, J. C. Campbell, B. E. A. Saleh, and M. C. Teich, "Optimized breakdown probabilities in $Al_{0.6}Ga_{0.4}As$-GaAs heterojunction avalanche photodiodes," *IEEE Electron Device Lett.*, vol. 25, no. 9, pp. 599–601, Sep. 2004.

Souye Cheong Liew Tat Mun received the M.Eng. degree in electronic engineering (computing) from the University of Sheffield, Sheffield, U.K., in 2004, where he is currently working toward the Ph.D. degree in electronic and electrical engineering.

His current research focused on the characterization and optimization of various infrared photodetectors.

Chee Hing Tan (M'05) received the B.Eng. and Ph.D. degrees in electronic engineering from the University of Sheffield, Sheffield, U.K., in 1998 and 2002, respectively.

Currently he is a Senior Lecturer with the Department of Electronic and Electrical Engineering. His research activities include experimental and theoretical investigation of excess noise, breakdown and jitter in APDs and SPADs, design of high-speed APDs and HPTs, and infrared photodetectors.

Simon J. Dimler received the M.Eng. degree in electronic and electrical engineering from the University of Sheffield, Sheffield, U.K., in 2004, where he is currently working toward the Ph.D. degree in electronic and electrical engineering.

His current research focused on developing circuits and measurement setups for the characterization of photodetectors.

Lionel J. J. Tan received the B.Eng. degree in electronic and electrical engineering from the University of Sheffield, Sheffield, U.K., in 2003, where he is currently working toward the Ph.D. degree in electronic and electrical engineering.

His doctoral research focuses on InP-based avalanche photodiodes and Geiger-mode avalanche photodiodes.

Jo Shien Ng (M'99) received the B.Eng. and Ph.D. degrees from University of Sheffield, Sheffield, U.K., in 1999 and 2003, respectively, in electrical and electronic engineering.

From 2003 to 2006, she was with the University of Sheffield and was responsible for characterization within the National Centre for III-V Technologies. She became a Royal Society University Research Fellow in October 2006, and her research interests include avalanche photodiodes, Geiger-mode avalanche photodiodes, and material characterization.

Yu Ling Goh (S'02) received the B.Eng. degree in electronic and electrical engineering from Imperial College, London, U.K., and the M.Eng.Sc. degree from Multimedia University, Malaysia. She is currently working toward the Ph.D. degree in electronic and electrical engineering at the University of Sheffield, Sheffield, U.K.

Her research interests include avalanche photodiodes, infrared detectors, and material characterization.

John P. R. David (SM'96) received the B.Eng and Ph.D. degrees in electronic engineering from the University of Sheffield, Sheffield, U.K., in 1976 and 1983, respectively.

He joined the Central Facility for III-V Semiconductors, University of Sheffield, in 1985, where he was responsible for the characterization activity. In 2001, he joined Marconi Optical Components (now Bookham Technologies), Devon, U.K., before returning to a Faculty position with the University of Sheffield in September 2002. He has authored or coauthored more than 250 papers published in various journals and conference proceedings, largely in the areas of III-V characterization, impact ionization, and avalanche photodiodes.